River Flow 2010 - Dittrich, Koll, Aberle & Geisenhainer (eds) - © 2010 Bundesanstalt für Wasserbau ISBN 978-3-939230-00-7

Investigation of Horizontal Coherent Structures in a Shallow Open-Channel Flow Using Velocity Signal Decomposition

A. Kanani, H. Ahmari & A.M. Ferreira da Silva
Department of Civil Engineering, Queen's University, Kingston, Ontario, Canada

ABSTRACT: This paper concerns the large-scale horizontal coherent structures (HCS's) in open-channel flows. In contrast to large-scale vertical coherent structures, HCS's have not yet been the focus of directed, systematic studies, and as a result the exact role they play in river morphodynamics remains elusive. This paper, which is to be viewed as an extension of da Silva and Ahmari (2009), reports some of the first measurements and results of an extensive laboratory study recently initiated by the authors as an attempt to develop an understanding of the characteristic scales, dynamics and consequences of HCS's. At these early stages of the research, our efforts, and thus this paper, are directed towards the establishment of the characteristic length- and time-scales of HCS's. The present analysis rests on a series of flow velocity measurements carried out in a 21m-long, 1m-wide laboratory channel, having a flat, sand bed. Two different techniques of signal decomposition are applied to the oscillograms of instantaneous flow velocity, collected throughout the flow domain, to reveal the aforementioned characteristic scales: "smoothening" of the velocity records through time-averaging; and Empirical Mode Decomposition (EMD) combined with Power Spectral Density (PSD) analysis. The filtered (or smoothed) oscillograms of instantaneous flow velocity were found to invariably exhibit cycles of fluctuation of velocity consistent with the presence of large-scale horizontal coherent structures, affecting (or occupying) the entire body of fluid. The average length traveled by HCS's from their "birth" location to the location of their disintegration (i.e. the horizontal burst length) was found to be ≈ 5.4 times the flow width. In view of the present results, and given the similarity between the horizontal burst length and the average length of alternate bars and the wave-length of meanders, strongly suggesting a relationship between them, it seems particularly worthwhile to pursue further research on HCS's.

Keywords: *Horizontal coherent structures (HCS's); Open-channel flow; Velocity signal decomposition; Burst period; Burst length*

1 INTRODUCTION

As is well-known, turbulence coherent structures exist in open-channel and river flows at a broad range of spatial and temporal scales. Even though much of the existing literature focuses on coherent structures (or the bursting fluid motion) in the wall region, the fact that bursting fluid motions (ejections and sweeps) are not restricted to the wall region, but that they exist also in the outer region as a manifestation of large-scale coherent structures in this region, was unequivocally established in some of the earlier works on organized turbulent motion and the related bursting phenomena (see e.g. Grass 1971, Hussain 1983, Talmon et al. 1986, Rashidi & Banerjee 1988). The large-scale coherent structures, which, following Hussain (1983), can be defined as the largest conglomeration of turbulent eddies which has a prevailing sense of rotation, are "born", grow so as to eventually occupy the entire body of fluid, and finally disintegrate or "die" (Yalin 1992). In this work, the term burst will be used to designate the evolution of a large-scale coherent structure during its life-span. In open-channel flows, the bursts can be vertical or horizontal (Yalin 1992, Utami & Ueno 1977). The coherent structures of the former rotate in the vertical $(x;z)$-planes of flow, those of the latter in the horizontal $(x;y)$-planes.

Several prominent researchers have since long expressed the view that large-scale coherent structures play an important role in sediment transport as well as in the formation and/or development of large-scale river morphological features. In particular, large-scale vertical coherent structures (VCS's) have been associated with the formation

and/or development of dunes, and large-scale horizontal coherent structures (HCS's) with the formation and/or development of bars and meanders (more on the topic in Yalin 1992, Yalin & da Silva 2001, Best 2005, etc.). However, in the absence of a proper understanding of the flow organization at the larger (river reach) scale and an adequate characterization of the macro-turbulent structures in river flows, the exact role played by these structures has throughout the years remained elusive (Roy et al. 2004). Indeed, only relatively recently have substantial research efforts started to be devoted to the development of a proper understanding of the dynamics and possible consequences of large-scale coherent structures in the context of river flows. However, as can be inferred from the reviews on the topic by Yalin (1992) and Nezu & Nakagawa (1993), as well as from Tamburrino & Gulliver (1999), Buffin-Bélanger et al. (2000), Shvidchenko & Pender (2001), Roy et al. (2004), Franca & Lemmin (2008), even though such efforts have resulted in considerable advances, all research on the topic so far has focused exclusively on VCS's.

As a result, the existing information on the dynamics and life-cycle of HCS's, which have not yet been the focus of any directed, systematic studies, remains rather hypothetical, and to a large extent based on generalizations of the life-cycle of VCS's. For this reason, any associations between HCS's and patterns of sediment transport and large-scale river forms, such as alternate bars and meandering, even though suggested in the literature, and most prominently by Yalin (1992) and Yalin & da Silva (2001) (see also da Silva 2006), cannot but be viewed as largely speculative.

Considering the aforementioned, and in an attempt to contribute to a better understanding of the size, dynamics and consequences of HCS's in the context of river flows, the writers have initiated an extensive laboratory study focusing on these structures. The objective of this paper is to report some of the measurements and results of the first phase of this study, aimed at establishing the characteristic time and length scales of HCS's. This paper is to be viewed as an extension of the recent work by da Silva & Ahmari (2009).

2 HORIZONTAL COHERENT STRUCTURES AND BURSTS: FUNDAMENTALS AND EXISTING HYPOTHESES

Before proceeding further, some pertinent fundamentals of horizontal coherent structures and existing hypotheses regarding their life-cycle are reviewed below. These are used to guide the experimental setup adopted in this work.

i) Although, as mentioned in the Introduction, horizontal coherent structures have not yet been the focus of directed research, there are reasons to believe that in their life-cycle they follow, *mutatis mutandi*, a sequence of events similar to that followed by VCS's, with the difference that they occur in a horizontal "flow ribbon" (Yalin 1992). But this means that HCS's are likely to originate at the "points" P near the banks and the free surface (Figure 1a), where the horizontal shear stresses τ_{xy} are the largest, and from there be conveyed by the mean flow away from the bank and downstream while growing in size, eventually evolving to "width-scale rolling structures". Once the lateral extent of HCS's becomes as large as the flow width B, they must be expected to interact with the opposite bank and disintegrate into a cascade of smaller and smaller eddies, the neutralized fluid mass returning to its original bank so as to arrive there at $t = T_H$, after travelling the distance λ_H. The "birth" and growth of any such structure would clearly be accompanied by the ejection of low momentum fluid which travels towards the opposite bank, while its disintegration, by high momentum fluid traveling towards the original bank (sweep).

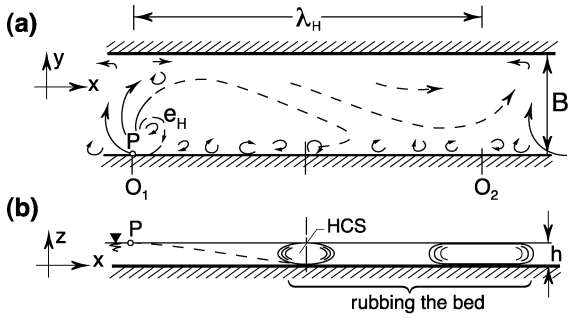

Figure 1. Conceptual representation of a horizontal burst-cycle. (a) Plan view; (b) Side view. HCS, horizontal coherent structure; e_H, eddy of horizontal turbulence

The prevailing view appears to be that the coherent structures forming the horizontal bursts of a wide open-channel have the shape of horizontally positioned disks, eventually extending (along z) throughout the flow thickness h (Yokosi 1967, Grishanin 1979, Jirka & Uijttewaal 2004, Yalin 2006).

The "break-up" of a coherent structure at any O_i prompts the birth of another at O_{i+1}. The distance O_iO_{i+1} between the "birth-places" of two consecutive bursts of a horizontal burst-sequence is the burst length λ_H, the life-span of a burst (i.e. the burst period) being $T_H = \lambda_H / v$, where v is the average flow velocity (for the coherent structures are transported by the flow with the velocity $\approx v$).

ii) Bursts are randomly distributed in space and time. This implies that under completely uniform conditions of flow, there is an equal probability (or frequency) of occurrence of bursts for any region Δx and time interval Δt. This applies to both vertical and horizontal bursts. As pointed out by Yalin (1992), pp. 70-71, such a homogeneous, or uniform, distribution of bursts along the flow direction x cannot lead to a wave-like deformation of the flow, in turn, capable of leading to a periodic deformation of the bed and/or banks. According to the just mentioned author, there must thus be in the flow a "location of preference" leading to the increment of the frequency of bursts at that location – and, since the break-up of one coherent structure (CS) triggers the "birth" of the next CS, leading also to the more frequent generation of sequences of bursts initiating from it. The perpetual action of such burst sequences on the flow must inevitably make it to acquire a periodic "deformation", ultimately leading to the periodic deformation of the bed surface. Yalin (1992) further argued that, in practice, an increased frequency of bursts at a location can be realized by means of a local discontinuity (the section containing it thus becoming the preferential section, $x = 0$ say). In the case of laboratory conditions, the discontinuity can be the beginning of the mobile bed or banks, an accidental ridge on the sand surface, etc.

iii) If, as hinted by Kishi (1980) and Jaeggi (1984), and as extensively argued by Yalin (1992) and Yalin & da Silva (2001), alternate bars are the "imprints" of HCS's on the bed, and since alternate bars are anti-symmetrical with respect to the x-axis (Figure 2c), in all likelihood so must be the sequences of horizontal bursts issued from the right and left banks, respectively. The likely anti-symmetrical arrangement of the sequences of bursts (which are supposed to initiate from a discontinuity in the sense of the previous paragraph) is shown in Figure 2a. [Note that Figure 2b shows the related periodic deformation of the flow streamlines.]

3 EXPERIMENTAL SET-UP AND FLOW CONDITIONS

The present flow velocity measurements were carried out in a 1m-wide, 21m-long and 0.4m-deep straight channel (see Figure 3). The channel was installed in a 21m-long, 7m-wide river basin equipped with a water re-circulation system, the complete details of which are given elsewhere (Ahmari 2010). The upstream end of the river basin consists of a 1.85m-wide and 8.8m-long stilling tank, a 0.60m-tall wall separating the stilling

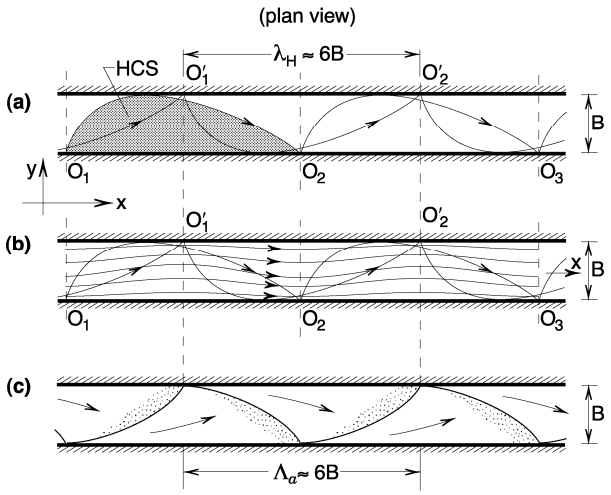

Figure 2. Plan view of straight channel showing: (a) Likely anti-symmetrical arrangement of horizontal coherent structures (HCS's); (b) Related internal meandering of flow; (c) Alternate bars on the movable bed. Λ_a, length of alternate bars.

tank from the river basin. The water entered the present experimental channel through a 1m-wide opening on this wall. The side walls of the channel were vertical and made of aluminum. The channel bed was formed by a well-sorted silica sand, with an average grain size D_{50} of 2mm. To ensure that the bed material would not be removed from the bed at the entrance of the experimental channel, a 1m-long stretch of gravel of diameter ≈ 2.5 cm was installed at the upstream end of the channel. The surface of the sand bed was scraped so as to produce the desired stream slope, and a flat bed surface. The flow free surface slope was adjusted by means of a tailgate at the end of the channel.

The hydraulic conditions of the turbulent, subcritical and uniform flow under investigation are summarized in Table 1, where B is the flow width, Q is the flow rate, h is the flow depth, S is the bed slope, Fr is the Froude number, Re is the flow Reynolds number, Re_* is the roughness Reynolds number ($= v_* k_s / \nu$, where $v_* = \sqrt{\tau_0 / \rho} = \sqrt{gSh}$ is the shear velocity and k_s is the granular skin roughness), and Y / Y_{cr} is the relative flow intensity ($Y = \tau_0 / (\gamma_s D)$ being the mobility number and Y_{cr} the value of Y at the critical stage (stage of inception of sediment transport)). Here the symbols τ_0 and γ_s stand for bed shear stress and submerged specific weight of the bed material, respectively.

Table 1. Hydraulic conditions of the flow under investigation (B=1m; D_{50}=2mm).

Q (l/s)	h (cm)	Fr	Re	Re_*	Y/Y_{cr}	B/h	h/D
9.0	4.0	0.36	9000	97	0.40	25	20

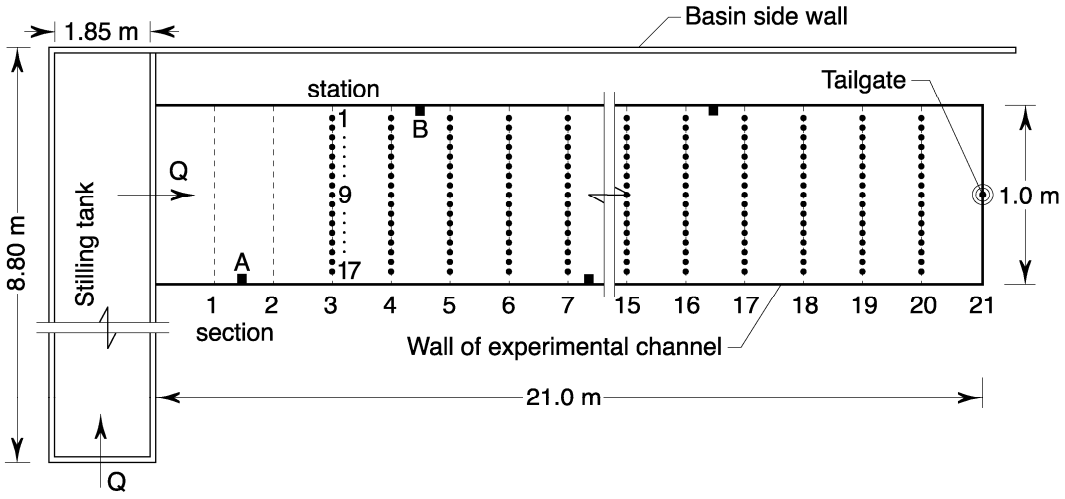

Figure 3. Schematic of experimental channel and location of velocity measurements (stations 1 to 17 in cross-sections 3 to 20)

For the present sand, Y_{cr} was identified with 0.045 while, following Kamphuis (1974) and Yalin (1977), k_s was identified with $2D_{50}$. The usual value of 16186.5 N/m^3 was adopted for the sand submerged specific weight γ_s. The value of the average flow velocity in the channel was $v = 22.5$ cm/s. Note that the bed shear stress acting on the bed was substantially below the threshold for initiation of motion – thus ensuring that the bed remained flat throughout the measurements.

The specific combination of the values of B, h and D of the present flow was selected so that the flow would lead to the occurrence of alternate bars provided that the material on the bed would be able to move. The present flow thus purposely plots well in the midst of the alternate bar region of the $(B/h; h/D)$-plan defining the existence regions of large-scale bed forms (alternate and multiple bars) and large-scale plan forms (meandering and braiding) due to da Silva (1991) (which can be found, in its most recent updated form, in Yalin & da Silva (2001) and da Silva (2006)).

In order to establish "location of preferences" for generation of bursts and bursts-sequences on both walls (see the previous section, paragraphs (ii) and (iii)), two 10cm-long blocks with 2cm×2cm square bases (blocks A and B) were attached to the walls, with their longest sides standing vertically and their square bases lying ≈2cm from the bed surface. The exact location of the blocks was as shown in Figure 3.

The measurements consisted of 2 minute-long records of instantaneous flow velocity collected at cross-sections 3 to 20 (Figure 3), and in each cross-section at 17 different points (henceforth referred to as stations). The stations were equally spaced along each cross-section, with stations 1 and 17 located 10cm from the channel walls. The sampling time to produce a complete set of 2min-long oscillograms of flow velocity was 10.2 hours (= 2 min per station times 306 measurement stations (17 stations per cross-section and 18 cross-sections)). All velocity measurements were carried out 1cm below the free surface with the aid of a SonTek 16MHz 2-D Micro ADV. This was operated at a sampling frequency of 20Hz (more on the topic in Ahmari 2010).

4 SIGNAL DECOMPOSITION

In order to identify the largest coherent structures in the flow, the records (oscillograms) of fluctuating flow velocity were treated with the aid of two different methods: a simple "smoothening" of the oscillograms through time-averaging; and empirical mode decomposition (EMD) of the records combined with power spectral density (PSD) analysis of the resulting decomposed velocity records.

4.1 *"Smoothening" of the fluctuating velocity oscillograms*

As indicated by e.g. Yokosi (1967), Yalin (1992), by averaging the oscillogram of the time-variation (due to turbulence) of flow velocity over consecutive time-intervals Δt, then the "smoothened" (or filtered) oscillograms contain only those velocity fluctuations whose period is larger than Δt. Thus, by selecting a sufficiently large Δt, it is possible to reveal those longest periods (or lowest frequencies) of the velocity fluctuations which are due to the largest structures in the flow, and thus to reveal the burst-period (Yalin 1992).

The procedure described in the previous paragraph to determine the longest periods of the velocity fluctuations is illustrated in Figure 4, using as example the 2min-long oscillogram of the fluc-

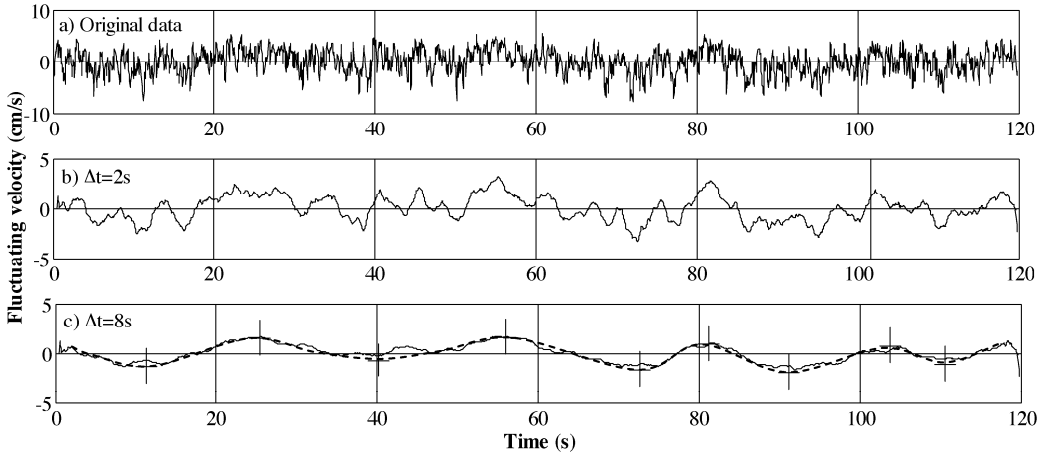

Figure 4. (a) Original 2min-long oscillogram of the fluctuating component of longitudinal flow velocity collected at section 10-station 17; (b) and (c) Resulting fluctuating velocity diagrams after averaging with the time-interval $\Delta t = 2s$ and $\Delta t = 8s$, respectively

tuating component of longitudinal flow velocity u' collected at section 10, station 17. Figure 4a shows the original oscillogram of u'; Figures 4b and 4c were obtained by using the consecutive averaging time-intervals of $\Delta t = 2s$ and $\Delta t = 8s$, respectively. In this example, the longest periods of the velocity fluctuations became evident when $\Delta t \approx 8s$. This can be inferred from Figure 4c, where the solid line is the smoothened oscillogram (and the dashed line is drawn so as to closely follow the trend of the smoothened oscillogram while highlighting the peaks and troughs of the oscillogram). Observe also from Figure 4c that the smoothened oscillogram in this example exhibits a rather regular cyclic pattern of variation, with four cycles between the troughs at $t \approx 11s$ and $t \approx 111s$. This yields, for this example, a value of $\approx 25s$ $(=(111-11)/4))$ as the average value (averaged over the sampling time of 2min) of the periods of velocity fluctuations due to the largest structures in the flow.

As a rule, it was found that an averaging time interval of 8*s* was adequate to reduce the oscillograms to the point where the periods of the fluctuations due to the largest structures in the flow were clearly evident.

4.2 *Empirical Mode Decomposition (EMD)*

Empirical Mode Decomposition (EMD), introduced by Huang et al. (1998), has been successfully applied to the study of turbulent flows in different fields. This includes the study of turbulent open-channel flow, as illustrated by the recent applications by Zeris & Prinos (2005), Huang et al. (2007) and Franca & Lemmin (2008). EMD adaptively decomposes a time series into its intrinsic mode functions (IMF's). An intrinsic mode function has the following two characteristics (Huang et al. 1998): 1- in the whole data set, the number of extrema and number of zero crossings must be equal or differ by 1; and 2- at any point, the mean value of the envelope defined by the local maxima and envelope defined by the local minima must be zero.

Huang et al. (2007) presented the following procedure to decompose a time series $x(t)$ into IMF's:

1- Find the local extrema of the signal $x(t)$.
2- Determine the upper envelope, $e_{\max}(t)$, of the signal by connecting the local maxima with the aid of a cubic spline interpolation. Determine also the lower envelope, $e_{\min}(t)$, of the signal by following a similar procedure.
3- Find the mean $m_1(t) = [e_{\max}(t) + e_{\min}(t)]/2$.
4- Determine the local detail $h_1(t)$ by subtracting the mean from the main signal.
5- Check whether $h_1(t)$ satisfies the required conditions to be an IMF, as stated above. If yes, then the resulting $h_1(t)$ is the first IMF. In this case, find the residual $r_1(t) = x(t) - C_1(t)$ and adopt it as the new series to which steps 1 to 5 are to be applied again to determine subsequent IMF's. If $h_1(t)$ is not an IMF, a procedure called "sifting process" is applied as many times as needed to obtain an IMF.
6- In the "Sifting process", start by adopting $h_1(t)$ as the new data; based on local extrema, determine its lower and upper envelopes, as well as their mean m_{11}. Then determine $h_{11}(t) = h_1(t) - m_{11}(t)$ and check whether or not $h_{11}(t)$ is an IMF. If not, the sifting process is repeated until $h_{1k}(t)$ satisfies the IMF conditions. In this case, the first IMF is $C_1(t) = h_{1k}(t)$, the residual $r_1(t) = x(t) - C_1(t)$ being taken as the new series in step 1.

The above procedure was adopted in this paper to decompose the velocity signals. As an example, some of the IMF's (namely IMF-1, IMF-3, IMF-5

and IMF-7) resulting from the application of EMD to the 2min-long oscillogram of the fluctuating component of longitudinal flow velocity u' collected at section 15, station 2, are shown in Figure 5. In total, the oscillogram was decomposed into 9 IMF's (not shown in their entirety here because of the limitations in paper size).

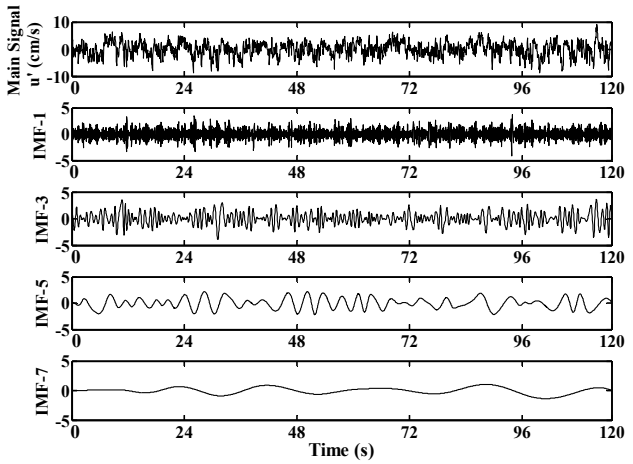

Figure 5. Example of main signal and decomposed signals (IMF's 1, 3, 5, and 7). Main signal in this figure is the oscillogram of fluctuating component of longitudinal flow velocity collected at section 15, station 2.

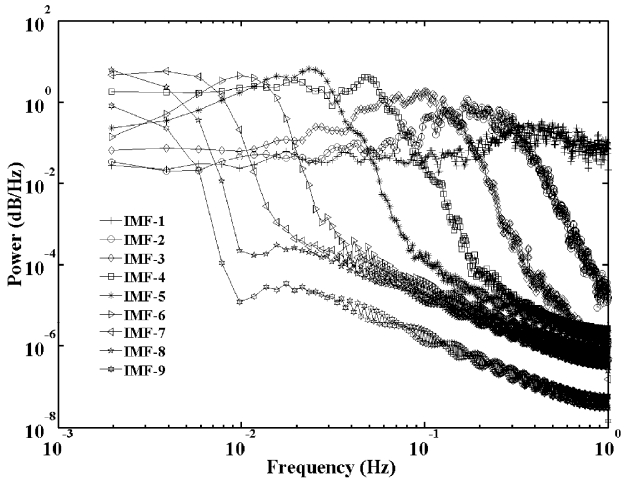

Figure 6. Power spectrum for resulting IMF's 1 to 9 at section 15, station 2

4.3 *Power spectrum*

In turbulent flow, different IMF's have different physical meanings (noise, small structures, large scale structures, etc.), and are thus associated with different characteristic frequencies (Huang et al. 2007). The power spectrum of a signal gives the distribution of the power of the signal among various frequencies and shows the existence, and also the relative power, of repetitive patterns and/or random structures in a signal (Vaseghi 2008). Considering this, in this paper, once a signal was decomposed into its intrinsic IMF's, the power (energy per unit time) spectrum of each IMF was determined. It was observed that, invariably, one IMF is found that, for some frequency, exhibits the highest (of all IMF's) power. Since this frequency is in line with the apparent frequency band of the HCS's, it is assumed that the HCS's are represented by this mode. Consequently, the burst period was determined as the inverse of the frequency corresponding to the highest contribution to power of such IMF. The method is illustrated in Figure 6, showing the power spectrum for the 9 IMF's resulting from the EMD at section 15, station 2 (partially shown in Figure 5). As can be inferred from Figure 6, among the nine IMF's, IMF-5 has the overall highest contribution to the power of the main signal, occurring at a frequency of ≈ 0.03 Hz, and corresponding to a period (horizontal burst-period) of ≈ 33.3 s.

5 RESULTS

For each of the present series of measurements, both of the techniques discussed in the previous section were applied to the entire set of 2min-long oscillograms of u', covering the flow domain from sections 3 to 20 (and collected in each section at stations 1 to 17).

i) After applying the "smoothening" procedure described in Section 4.1 to all of the measured oscillograms, each of the smoothened oscillograms was then used to determine the average value of the periods of its velocity fluctuations (averaged over the sampling time of 2min). The ranges of variation of such average values for the entire sets of 2min-long oscillograms as well as the frequency of occurrence of specific values within such ranges, can be inferred from the frequency plots in Figure 7. These plots are presented in the form of probability density plots with the solid line representing the pdf of a fitted normal distribution. For the purpose of producing these plots, the channel was divided into the following three regions: an upstream region, from sections 3 to 7, a middle region, from sections 8 to 14, and a downstream region, from sections 15 to 20.

Irrespective of location in flow domain, the smoothened oscillograms were found to invariably exhibit long cycles of increasing/decreasing/increasing u', by multiple times larger than those that can be expected because of large-scale vertical coherent structures. Indeed, the burst length of the largest vertical structures λ_V is known to be of the order of $\approx 6h$ (see e.g. Jackson 1976, Yalin 1992; Roy et al. 2004). Thus, for the present flow they are associated with periods of $\approx 1s$ ($T_V = \lambda_V / v = (6 \cdot 0.04)/0.225 \approx 1s$). Yet, the duration of each cycle of fluctuation of u' in the present smoothened oscillograms was at its

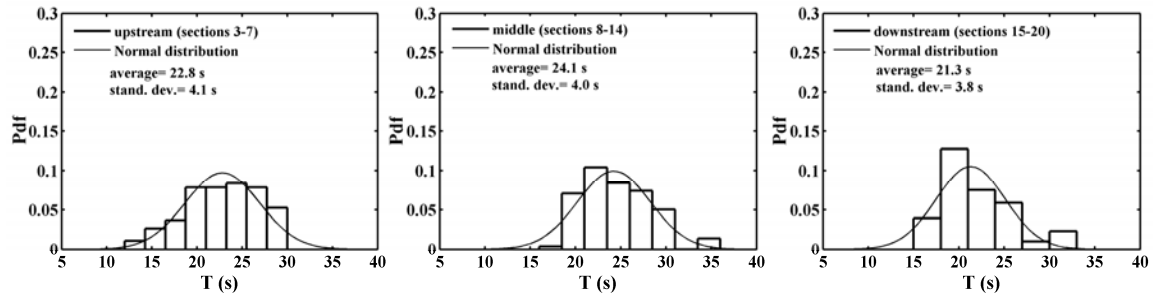

Figure 7. Probability density plots of the average values of the periods of velocity fluctuations of the smoothened oscillograms of fluctuating velocity. The plots are divided into upstream region of the channel (sections 3 to 7), middle region (sections 8 to 14) and downstream region (sections 15 to 20). The values of average and standard deviation shown are those of the fitted normal distribution.

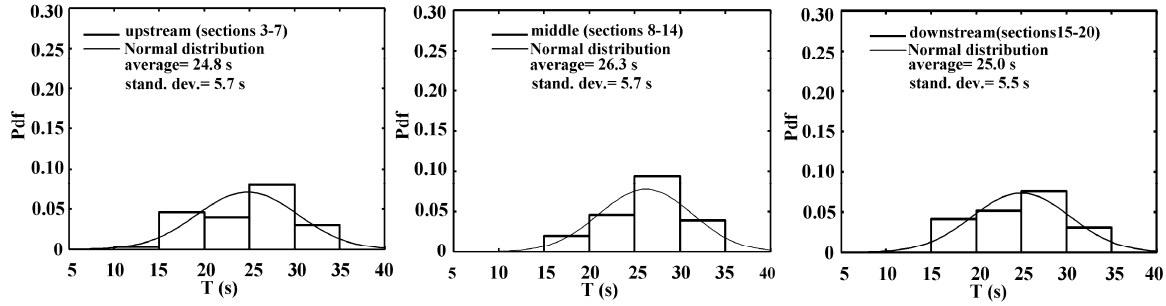

Figure 8. Probability density plots of the resulting values of the characteristic period of "dominant" IMF obtained with the aid of EMD combined with PSD analysis. The plots are divided into the same channel regions as in Figure 7. The values of average and standard deviation shown are those of the fitted normal distribution.

minimum of the order of ≈ 5 to $10s$, say, and in fact, as a rule much larger than $10s$.

The large duration of the individual cycles of velocity fluctuation in the smoothened oscillograms, and the fact that such cycles are present in all of the oscillograms, irrespective of their location in the flow domain, cannot but be viewed as an indication of the presence of large-scale horizontal turbulence structures, affecting (occupying) the entire body of fluid. Moreover, the regularity ("periodicity") in the cycles of velocity increase/decrease/increase of the smoothened oscillograms, and the fact that such regularity can be found throughout much of the channel, is consistent with the presence of large-scale periodic events in the flow, and more specifically with the presence of persistent horizontal burst-sequences originating at (or promoted by) the discontinuities.

ii) After applying EMD and PSD, as described in Sections 4.2 and 4.3, to each individual oscillogram of fluctuating flow velocity to reveal "its" horizontal burst-period, the frequency plots shown in Figure 8 were produced. Just like in Figure 7, these are presented in the form of probability density plots with the solid line representing the pdf of a fitted normal distribution.

iii) An estimate of the value of the (average) burst period T_H of the bursts in the burst-sequences issued from the discontinuities is provided here by identifying T_H with the average of the mean values of the fitted distributions in the six diagram in Figures 7 and 8 (namely 22.8, 24.1, 21.3, 24.8, 26.3 and 25s). This yields for the average burst period $T_H \approx 24s$. Using this value, one obtains for the average burst length $\lambda_H = v \cdot T_H \approx 5.4m$ (where $v = 0.225m/s$ is the average flow velocity), and thus $\lambda_H / B \approx 5.4$.

6 CONCLUDING REMARKS

The main results of this work can be summarized as follows:

1- The filtered (or smoothed) oscillograms of u' throughout the flow domain were found to invariably exhibit cycles of fluctuation of velocity consistent with the presence of large-scale horizontal coherent structures, affecting (or occupying) the entire body of fluid. The cycles of fluctuation of u' also suggested that these were part of horizontal burst-sequences promoted by discontinuities.

2- As discussed by Yalin (1992), pp. 70-71, the sequences of bursts promoted by the upstream discontinuities must necessarily be expected to attenuate along the flow direction x. That is, the conditions sufficiently far from the discontinuities must eventually revert to those that would be observed in the absence of any discontinuities. How-

ever, the present channel was comparatively short, and the horizontal burst-sequences appeared to remain "intact" throughout the channel, with their signal still quite evident in the velocity records at the downstream end of the channel.

3- The average burst-length λ_H (normalized by the flow width B) of the aforementioned burst-sequences was found to be $\lambda_H / B \approx 5.4$. The proportionality factor between λ_H and B, namely 5.4, is comparable to the proportionality factor relating the length of alternate bars and the wavelength of meanders to the flow width (see Yalin & da Silva 2001 and da Silva 2006). This finding lends support to the longstanding belief expressed by many prominent researchers that the formation of large-scale river forms, and in particular alternate bars and meanders, are related to the large-scale turbulence.

ACKNOWLEDGMENTS

This research was supported by funds from the Natural Sciences and Engineering Research Council of Canada and the Ontario Research and Development Challenge Fund.

REFERENCES

Ahmari, H. 2010. Size, dynamics and consequences of large-scale horizontal coherent structures in open-channel flows: an experimental study. Ph.D. Thesis, Queen's University, Kingston, Canada.

Best, J. 2005. The fluid dynamics of river dunes: a review and some future research directions. J. Geophys. Res., 110: F04S02.

Buffin-Bélanger, T., Roy, A.G. and Kirkbride, A.D. 2000. On large-scale flow structures in a gravel-bed river. Geomorphology, 32: 417-435.

da Silva, A.M.F., and Ahmari, H. 2009. Size and effect on the mean flow of large-scale horizontal coherent structures in open-channel flows: an experimental study. Special Issue in Honour of Professor M. Selim Yalin, CJCE, Vol. 36(10): 1643-1655.

da Silva, A.M.F. 2006. On why and how do rivers meander. 14th IAHR Arthur Thomas Ippen Award Lecture, J. Hydr. Res., 44(5): 579-590.

da Silva, A.M.F. 1991. Alternate bars and related alluvial processes. M.Sc. Thesis, Queen's University, Kingston, Canada.

Franca, M. J., and Lemmin, U. 2008. Using empirical mode decomposition to detect large-scale coherent structures in river flow. Proc. River Flow 2008: 67-74.

Grass, A.J. 1971. Structural features of turbulent flow over smooth and rough boundaries. J. Fluid Mech., 50(2): 233-255.

Grishanin, K.V. 1979. Dynamics of alluvial streams. (In Russian) Gidrometeoizdat, Leningrad.

Huang, N., Shen, Zh., Long, S., Wu, M., Shih, H., Zheng, Q., Yen, N., tung, C., and Liu, H.,1998. The empirical mode decomposition and the Hilbert spectrum for nonlinear and non-stationary time series analysis. Proc., R. Soc. Lond., England: 909-995.

Huang, Y., Schmitt, F., Lu, Zh., and Liu, Y. 2007. Empirical mode decomposition analysis of experimental homogeneous turbulence time series. Colloque GRETSI; 11-14 September 2007, France, Troyes.

Hussain, A.K.M.F. 1983. Coherent structures – reality and myth. Phys. Fluids, 26: 2816-2838.

Jackson, G. 1976. Sedimentological and fluid-dynamic implications of the turbulent bursting phenomenon in geophysical flows. J. Fluid Mech., 77: 531-560.

Jaeggi, M. 1984. Formation and effects of alternate bars. J. Hydr. Engrg., ASCE, 110(HY2).

Jirka, G.H.,, and Uijttewaal, W.S.J. eds. 2004. Shallow flows: selected papers of the Int. Symposium on Shallow Flows, 16-18 June 2003, Delft, The Netherlands, A.A. Balkema, Rotterdam, The Netherlands.

Kamphuis, J.W. 1974. Determination of sand roughness for fixed beds. J. Hydraul. Res., 12(2): 193-203.

Kishi, T. 1980. Bed forms and hydraulic relations for alluvial streams. In Application of Stochastic Processes in Sediment transport, H.W. Shen and H. Kikkawa eds., Water Resources Publications, Litleton, Colorado.

Nezu, I., and Nakagawa, H. 1993. Turbulence in open-channel flows. IAHR Monograph, A.A. Balkema, Rotterdam, The Netherlands.

Rashidi, M., and Banerjee, S. 1988. Turbulence structures in free-surface channel flows. Phys. Fluids, 31(9): 2491-2501.

Roy, A.G., Buffin-Bélanger, T., Lamarre, H., and Kirkbride, A.D. 2004. Size, shape and dynamics of large-scale turbulent flow structures in a gravel-bed river. J. Fluid Mech., 500: 1-27.

Shvidchenko, A. B., and Pender, G. 2001. Macroturbulent structure of open-channel flow over gravel beds. Water Resour. Res., 37(3): 709–719.

Talmon, A.M., Kunen, J.M.G., and Ooms G. 1986. Simultaneous flow visualization and Reynolds-stress measurement in a turbulent boundary layer. J. Fluid Mech., 163: 459- 478.

Tamburrino, A., and Gulliver, J.S. 1999. Large flow structure in a turbulent open channel flow. J. Hydr. Res., 37(3): 363-380.

Utami, T., and Ueno, T. 1977. Lagrangian and Eulerian measurement of large-scale turbulence. In Flow Visualization I. Proc. Int. Symp. On Flow Visualization, Asanuma, T. (ed.), Hemisphere, Washington.

Vaseghi, A. 2008. Advanced digital signal processing and noise reduction. 4th Edition, John Wiley and Sons Ltd Publication.

Yalin, M.S. 2006. Large-scale turbulence and river morphology. Proc. River Flow 2006, 3rd International Conference on Fluvial Hydraulics, Lisbon, Sept. 6-8, Ferreira, Alves, Leal & Cardoso (eds.), Taylor & Francis Group, London: 1243-1249.

Yalin, M.S., and da Silva, A.M.F. 2001. Fluvial processes. IAHR Monograph, IAHR, The Netherlands.

Yalin, M.S. 1992. River mechanics. Pergamon Press, Oxford.

Yalin, M.S. 1977. Mechanics of sediment transport. Pergamon Press, Oxford.

Yokosi, S. 1967. The structure of river turbulence. Bull. Disaster Prevention Res. Inst., Kyoto Univ., Vol. 17, Part 2, No. 121, Oct.: 1-29.

Zeris, A., Prinos, P. 2005. Coherent structures analysis in turbulent open channel flow using Hilbert-Huang and Wavelets transforms. Taylor and Francis Group LLC. Boca Raton, USA.